Visible-Light Induced Photocatalysis of Partially Fluorinated Poly(*p*-phenylene) and Related Linear Phenylene Derivatives

Katsuya MARUO, Kazuyori YAMADA, Yuji WADA, and Shozo YANAGIDA*
Chemical Process Engineering, Faculty of Engineering, Osaka University, Suita, Osaka 565
(Received November 6, 1992)

As a partially fluorinated poly(*p*-phenylene) derivative, yellow powder PF-PPP-*n* with high solubility in organic solvents was prepared as a mixture of oligomers by nickel-catalyzed polycondensation of the Grignard reagent from 1-bromo-2,4,6-trifluorobenzene. PF-PPP-*n* shows photocatalytic activity for reduction of water to H_2, carbonyl compounds to alcohols, and dimethyl maleate and fumarate to the succinate under visible-light ($\lambda > 400$ nm) irradiation in the presence of triethylamine as a sacrificial electron donor. The photocatalysis was compared with those of other related fluorinated linear aromatics such as perfluorinated poly(*p*-phenylene sulfide) (F-PPS-*n*), perfluorinated poly(*p*-phenylene) (F-PPP-*n*). Their spectral characteristics and photocatalysis are discussed on the basis of the semiempirical molecular orbital calculations.

In the previous paper,[1] we reported novel photocatalytic properties of perfluorinated oligo(*p*-phenylenes) (F-OPP-*n*), and successfully rationalized their physical properties and photochemical reactivity by semiempirical molecular orbital (MO) calculations in comparison with those of unfluorinated oligo(*p*-phenylenes) (OPP-*n*). Perfluorinated *p*-terphenyl (F-OPP-3) can induce photoreduction of water to H_2 in the presence of triethylamine (TEA) as a sacrificial electron donor and noble metal colloids as an electron mediator under UV irradiation. In this system, F-OPP-3 is supposed to be converted into its anion radical, which reduces protons to H_2 through noble metal mediators as well as OPP-3. However, F-OPP-$3^{-\bullet}$ was found to degrade in the photoreduction system. The photoreductive degradation of F-OPP-3 can be predicted by taking into account spin localization in the anion radical as calculated by the semiempirical MO calculation. On the other hand, F-OPP-3 exhibited photocatalytic activity for oxidation of benzene to phenol in aqueous acetonitrile in the presence of O_2 under UV ($\lambda > 290$ nm) irradiation, while OPP-3 was inactive for this reaction. It was proposed that the radical cation of F-OPP-3, i.e., F-OPP-$3^{+\bullet}$, plays a critical role to oxidize benzene molecule to phenol in the photooxidation system. The stronger oxidizing power of F-OPP-$3^{+\bullet}$ compared to OPP-$3^{+\bullet}$ was rationalized by the MO calculation. It enables F-OPP-3 to function as an organic photooxidation catalyst. The semiempirical MO calculation using the MOPAC system (MNDO/PM3) also reveals that the strength of the C–F bond is strengthened in the cation radical, the neutral molecule, and the anion radical, explaining the high stability of F-OPP-3 in the photooxidation system.

The above facts led us to the idea that the characterization of oligomeric linear aromatics and their intermediary radical species by means of the semiempirical MO calculation is useful for the molecular design of organic photocatalysts and the precise control of their photocatalytic properties.

With this in mind, we aimed at developing novel photocatalysts that are derived from fluorinated linear aromatics, and that absorb in the visible light region. The MO calculation revealed that the steric repulsion between fluorine atoms in F-OPP-*n* should increase the angle of torsion between the perfluorinated benzene rings, leading to a hypsochromic shift of the onset of the absorption spectrum compared with OPP-*n*.[1] For the present study on photocatalysis driven by visible-light ($\lambda > 400$ nm) irradiation, we selected two methods to relax the steric repulsion; the first is the partial fluorination of *p*-phenylene (PF-PPP-*n*, partially fluorinated poly(*p*-phenylene)) (see Scheme 1) and the second is to introduce sulfur as a spacer between the neighboring phenylene rings of perfluorinated poly(*p*-phenylene) (F-PPP-*n*), i.e., poly(*p*-phenylene sulfide) (F-PPS-*n*).[2] In this paper, we report photocatalysis of partially fluorinated poly(*p*-phenylene) (PF-PPP-*n*) in comparison with that of some related linear aromatics (Scheme 1). In addition, a semiempirical molecular orbital calculation using the MOPAC system (MNDO/PM3 and MNDO/AM1) was applied to theoretically analyze the photocatalysts and their intermediately formed radicals.

Result and Discussion

Preparation and Characterization of Partially Fluorinated Poly(*p*-phenylene) (PF-PPP-*n*) and Related Fluorinated Linear Aromatics. PF-PPP-*n* was prepared according to Yamamoto's method,[3] i.e., by polymerization of the Grignard reagent obtained from 1-bromo-2,4,6-trifluorobenzene as shown in Scheme 2. The resulting PF-PPP-*n* was found to be soluble even in methanol to an appreciable extent (about 0.017 g ml^{-1}), and was therefore purified by reprecipitation in aqueous methanol. PF-PPP-*n* thus obtained was found to be oligomeric ($n > 3$) comparable to PPP-*n* obtained in a similar way as confirmed by GPC and mass spectral analysis (see Experimental section). However, the longer oligomers ($n > 10$) could not be analyzed by mass spectral analysis due to the limit of the instrument used.

F-PPS-*n* was prepared by polymerization of potas-

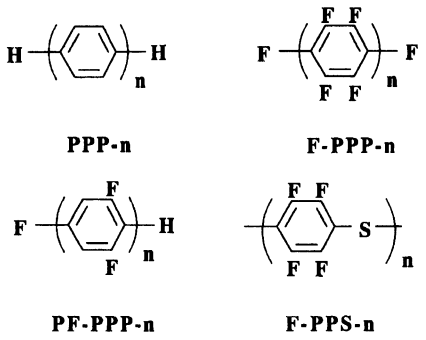

Scheme 1.

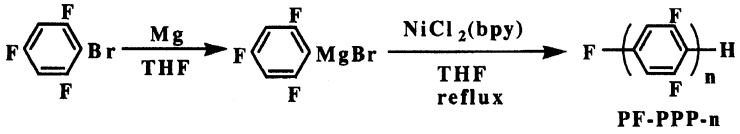

Scheme 2.

sium pentafluorobenzenethiolate in the presence of hexafluorobenzene in pyridine as shown in Scheme 3.[2] The precipitated F-PPS-n was collected and purified by washing with water several times, and mass spectral analysis revealed that the resulting F-PPS-n should consist of oligomers ranging from at least $n=6$ to $n=10$.

F-PPP-n was prepared by polymerization of pentafluorophenylmagnesium bromide and decafluorobiphenyl as shown in Scheme 4.[4] The insoluble F-PPP-n was purified the same way and analyzed by mass spectrometry. F-PPP-n was found to consist of oligomers ranging from at least $n=3$ to $n=10$.

Spectral Characteristics. Figure 1 shows the reflectance spectra of powders of the five compounds, i.e., PPP-n, F-PPP-n, PF-PPP-n, F-PPS-n, and PPS-n, measured by using a multichannel photodiode (MCPD) system. The onsets of the absorption spectra and their maxima are listed in Table 1. The onset wavelength for F-PPP-n (340 nm) was found at a much shorter wavelength than that for PPP-n (630 nm), implying that perfluorination of PPP-n causes a shift of the absorption to shorter wavelengths. This can be ascribed to the steric repulsion between fluorine atoms on neighboring phenylene rings.

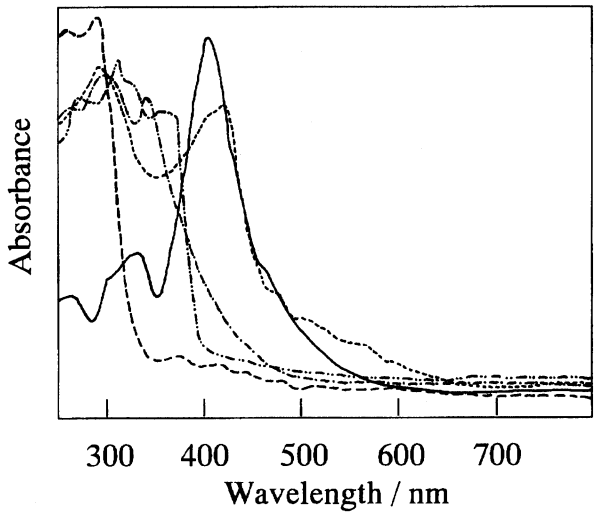

Fig. 1. Reflectance spectra of fluorinated and nonfluorinated linear aromatics: —, PF-PPP-n; ---, F-PPP-n; ····, PPP-n; -·-, F-PPS-n; -···-, PPS-n.

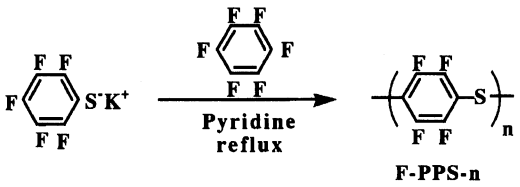

Scheme 3.

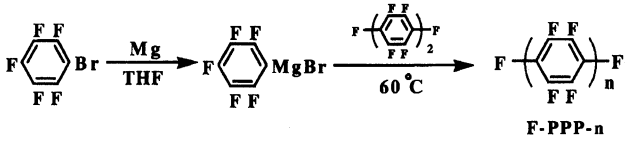

Scheme 4.

On the other hand, PF-PPP-n showed strong absorption in the visible region, the onset being shifted back to longer wavelengths. This suggests a success in relaxing the steric repulsion between fluorine atoms on the neighboring phenylene rings. This rationalization is supported by the fact that the introduction of substituents at ortho position of p-phenylene derivatives causes a hypsochromic shift, and the bulkier the substituents are, the more the shift becomes.[5a,5b] It is worth noting, however, that the introduction of four fluorine atoms into the central benzene ring of p-terphenyl (OPP-3), which gives 2′,3′,5′,6′-tetrafluoro-p-terphenyl,

Table 1. Onsets and Maxima of Reflectance Absorption Spectra of Fluorinated and Unfluorinated Phenylene Derivatives[a)]

	Onset of absorption/nm	Maxima of absorption/nm
PPP-*n*	630	420
F-PPP-*n*	340	285
PF-PPP-*n*	550	405
F-PPS-*n*	460	300
PPS-*n*	390	305

a) Measured by using MCPD system.

does not cause any change in the absorption maxima compared with that of OPP-3.[5c)]

F-PPS-*n* showed an onset of absorption at a longer wavelength than F-PPP-*n*. When compared with commercially available PPS-*n* (a typical number for the average molecular weight is 10000), F-PPS-*n* shows a comparable absorption spectrum, although the onset shifts slightly to longer wavelengths. These facts suggest that the insertion of a sulfur spacer between the *p*-phenylene rings was effective for the relaxation of the F–F repulsion leading to the bathochromic shift.

Photocatalysis of Water Reduction. In order to examine visible-light induced photocatalysis, photoreductions of water with PF-PPP-*n* or F-PPS-*n* were carried out using a 300-W halogen lamp fitted with a sodium nitrite solution filter ($\lambda > 400$ nm). Triethylamine (TEA) and $RuCl_3$ were chosen as sacrificial electron donors and a source of Ru metal as an electron mediator in the same way as reported for PPP-*n*[6a)] and poly(2,5-pyridinediyl) (PPy-*n*).[6b)] PF-PPP-*n* showed efficient photocatalytic activity for reduction of water to H_2, the efficiency being higher than that of PPP-*n* as shown in Fig. 2. PF-PPP-*n*-catalyzed H_2 evolution never occurred in the absence of either TEA, a noble metal source, or light-irradiation.

When $RhCl_3$ was used instead of $RuCl_3$, PF-PPP-*n* showed more efficient photocatalytic activity as observed in the case of perfluorinated *p*-terphenyl (F-OPP-3).[1)] The leveling-off in H_2 evolution was observed after 3—4 h irradiation, indicating gradual photodecomposition of PF-PPP-*n* as was observed for F-OPP-3 and OPP-3.[1,7)] With regard to F-PPS-*n*, however, H_2 evolution was negligible although it absorbs light in visible-region as shown in Fig. 1.

In order to compare the photocatalytic activity for H_2 evolution between five π-conjugated polymers, i.e., PF-PPP-*n*, F-PPP-*n*, F-PPS-*n*, PPP-*n*, PPS-*n*, the water photolysis was carried out under irradiation at $\lambda > 290$ nm in the presence of $RhCl_3$ as the source of an electron mediator, Rh (Fig. 3). At the initial stage in the photoreaction, $RhCl_3$ should be photoreduced through an electron transfer from anion radical of the π-conjugated polymer, giving Rh^0. It was therefore concluded that Rh^0 should mediate an electron transfer from anion radical of the π-conjugated polymer to a proton and/or water, as were observed for the OPP-*n* system.[7)]

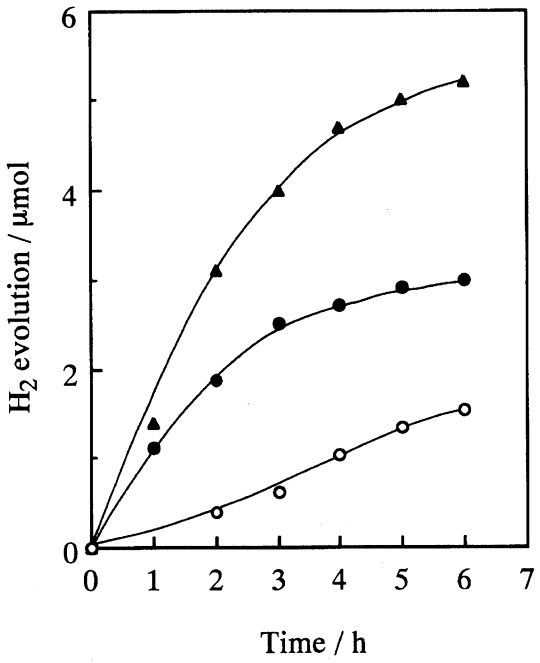

Fig. 2. Water-photoreductive H_2 evolution catalyzed by PF-PPP-*n* and PPP-*n* under irradiation with $\lambda > 400$ nm using $RuCl_3$: (●) PF-PPP-*n*; (○) PPP-*n*; (▲) PF-PPP-*n* (with $RhCl_3$).

It has now been found that PF-PPP-*n* shows the most efficient photocatalytic activity of the polymers examined under UV irradiation, the activity decreasing in the order PF-PPP-*n* > PPP-*n* > F-PPP-*n* ≫ F-PPS-*n* > PPS-*n*. F-PPS-*n* as well as PPS-*n* showed only miner activity under UV ($\lambda > 290$ nm) irradiation. It is worth noting that PF-PPP-*n* induced H_2 evolution occurred without leveling-off during 5 h of UV irradiation. With regard to the effective photocatalysis of PF-PPP-*n*, it should be mentioned that PF-PPP-*n* has a surprisingly high solubility in organic solvent such as methanol and THF. The high activity of PF-PPP-*n* can also be ascribed to homogeneous photocatalysis through dissolved PF-PPP-*n*, since PF-PPP-*n* is soluble to some extent in aqueous methanol, F-PPP-*n*, PPP-*n*, and F-PPS-*n* acting totally as heterogeneous photocatalysts.[7)]

Photocatalysing the Reduction of Aromatic Ketones. It has now been found that PF-PPP-*n* catalyzes the photoreduction of carbonyl compounds under irradiation with $\lambda > 400$ nm in the presence of TEA

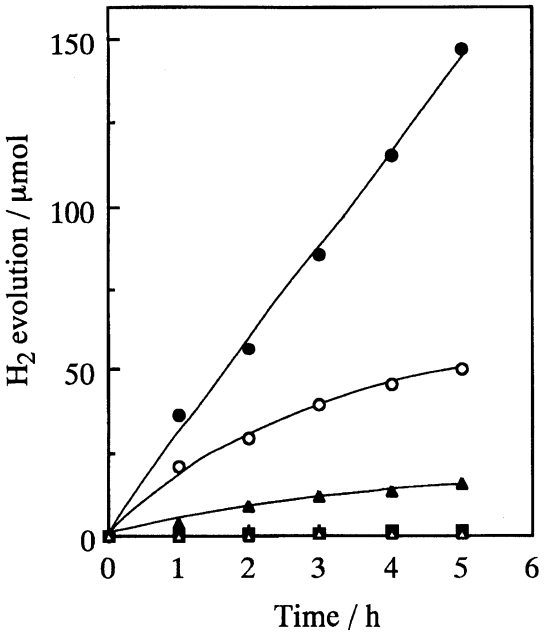

Fig. 3. Water-photoreductive H_2 evolution catalyzed by PF-PPP-*n*, F-PPP-*n*, F-PPS-*n*, PPP-*n*, and PPS-*n* under irradiation with $\lambda>290$ nm using $RhCl_3$: (●) PF-PPP-*n*; (▲) F-PPP-*n*; (■) F-PPS-*n*; (○) PPP-*n*; (△) PPS-*n*.

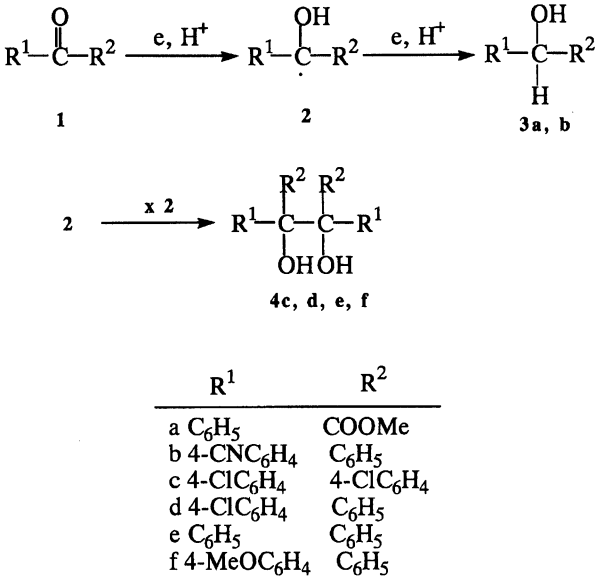

	R^1	R^2
a	C_6H_5	COOMe
b	4-CNC_6H_4	C_6H_5
c	4-ClC_6H_4	4-ClC_6H_4
d	4-ClC_6H_4	C_6H_5
e	C_6H_5	C_6H_5
f	4-$MeOC_6H_4$	C_6H_5

Scheme 5.

as an electron donor as do PPP-*n* and PPy-*n*.[6] Figure 4 shows the time-conversion plots for the PF-PPP-*n*-catalyzed photoreduction of methyl benzoylformate in methanol (a) and in acetonitrile (b). In both cases, methyl benzoylformate is reduced to methyl mandelate almost quantitatively. The reaction rate is faster in acetonitrile than in methanol.

The PF-PPP-*n*-catalyzed photoreduction was extended to other aromatic ketones with different reduction potentials both in methanol and in acetonitrile (Table 2). The carbonyl compound with reduction potentials comparable to methyl benzoylformate, e.g., *p*-cyanobenzophenone was photoreduced quantitatively and selectively to the corresponding alcohols both in methanol and in acetonitrile as shown in Scheme 5. However, the photoreduction of other carbonyl derivatives with reduction potentials more negative depends strongly on the solvent. In methanol, the substrates with reduction potentials more positive than −1.6 V vs. SCE were reducible to pinacols, the coupling products of one-electron-transfer reduction intermediates (**2**) (Scheme 5). On the other hand, in acetonitrile the carbonyl compounds were reduced exclusively to the corresponding alcohols. The threshold value of the reduction potential in acetonitrile was estimated to be around −1.9 V vs. SCE. The rate and the selectivity in PF-PPP-*n*-catalyzed photoreductions observed contradict those found for the PPP-*n*-catalyzed photoreductions of carbonyl compounds; the photocatalysis of PPP-*n* is much more effective in methanol than in acetonitrile, and the selectivity in the formation of either alcohols or pinacols was not affected by the solvent as exemplified in the 6 h photoreduction of benzophenone (Table 2), though the threshold value of the reduction potential is more negative (around −1.75 V vs. SCE in methanol) than PF-PPP-*n*.[6a]

The visible-light induced photoreduction of some carbonyl compounds was also examined using F-PPS-*n* or PPS-*n* as photocatalysts. Only methyl benzoylformate and di-2-pyridyl ketone were found to be reduced, yielding exclusively the corresponding alcohol (Table 3), while no photoreduction was observed when PPS-*n* was used instead of F-PPS-*n*. However, F-PPS-*n* showed no catalytic activity in methanol for substrates with reduction potentials more negative than −1.2 V vs. SCE.

Photoreduction of Dimethyl Maleate and Fumarate. Parts a and b of Fig. 5 show time plots of the PF-PPP-*n*-catalyzed photolysis of dimethyl maleate in methanol and in acetonitrile, respectively, using TEA as electron donor under visible-light ($\lambda>400$ nm) irradiation. Dimethyl maleate undergoes cis–trans photoisomerization, being sequentially photoreduced to dimethyl succinate in both solvents. Parts c and d of Fig. 5 depict the corresponding photolysis of dimethyl fumarate in methanol and in acetonitrile, respectively. Dimethyl fumarate was photoreduced to dimethyl succinate without cis–trans photoisomerization. The reduction potentials of dimethyl maleate and fumarate are 1.60 and 1.56 V vs. SCE in methanol,[8a] which are very close to the reduction threshold for the PF-PPP-*n*-catalyzed photoreduction. However, the photolysis proceeded well especially in acetonitrile as observed for the photoreduction of carbonyl compounds. The rates of conversion were about 5 times faster in acetonitrile than in methanol. All of the time-conversion plots indicate

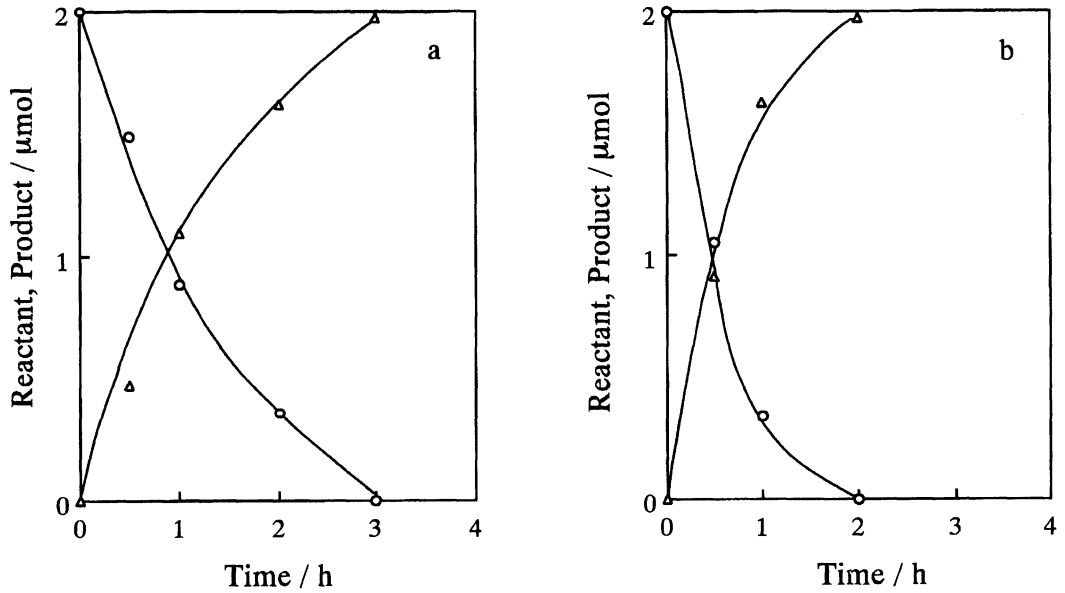

Fig. 4. Time-conversion plots for the PF-PPP-*n*-catalyzed photoreduction of methyl benzoylformate (a) in methanol; (b) in acetonitrile; (○) methyl benzoylformate; (△) methyl manderate.

Table 2. PF-PPP-*n*-Catalyzed Photoreduction of Aromatic Ketones with TEA[a)]

(R^1–CO–R^2)		Solvent	$-E^{red}_{1/2}$/V[b)]	Catalyst	Conversion/%	Yield[c)]/%	
R^1	R^2					Alcohol	Pinacol
Ph	CO_2Me	MeOH	1.13[d)]	PF-PPP-*n*	100[e)]	100	Trace
				PPP-*n*	98[e)]	74	Trace
4-CNPh	Ph	MeOH	1.17[f)]	PF-PPP-*n*	98	87	Trace
4-ClPh	4-ClPh	MeOH	1.31[g)]	PF-PPP-*n*	18	Trace	76
4-ClPh	Ph	MeOH	1.32[f)]	PF-PPP-*n*	12	0	89
Ph	Ph	MeOH	1.55[f)]	PF-PPP-*n*	6	0	65
				PPP-*n*	97	45	55
4-MeOPh	Ph	MeOH	1.56[f)]	PF-PPP-*n*	Trace	0	Trace
Ph	CO_2Me	AN[h)]	1.64[i)]	PF-PPP-*n*	100[e)]	100	0
4-CNPh	Ph	AN	1.42[j)]	PF-PPP-*n*	100	100	0
4-ClPh	4-ClPh	AN	1.67[j)]	PF-PPP-*n*	86	87	4
4-ClPh	Ph	AN	1.75[j)]	PF-PPP-*n*	100	88	0
Ph	Ph	AN	1.83[j)]	PF-PPP-*n*	37	75	19
				PPP-*n*	47	57	28
4-MeOPh	Ph	AN	—	PF-PPP-*n*	16	Trace	88
4-MeOPh	4-MeOPh	AN	2.02[j)]	PF-PPP-*n*	0	0	0

a) Irradiated with $\lambda > 400$ nm for 6 h. b) Polarographic half-wave reduction potentials in Volts vs. SCE in methanol or acetonitrile. c) Based on the converted substrate. d) See Ref. 6b. e) Irradiated with $\lambda > 400$ nm for 3 h. f) See Ref. 8a. g) Polarographic half-wave reduction potentials in Volts vs. NCE in 46% ethanol solution. See Ref. 8b. h) Acetonitrile. i) Polarographic half-wave potentials in Volts vs. $Ag/AgNO_3$ in acetonitrile. See Ref. 9a. j) See Ref. 8c.

that the disappearance of the starting substrates is not consistent with the formation of the reduction products, implying that inevitable side reaction through intermediary radical species from the substrates and TEA used as an electron donor play a major role.[10)]

Attempt to Photooxidize Benzene to Phenol using PF-PPP-*n* or F-PPS-*n*. We previously reported that F-OPP-3 catalyzes the photo-hydroxylation of benzene to phenol in aqueous acetonitrile in the presence of O_2 under UV ($\lambda > 290$ nm) irradiation.[1)] The same photooxidation was attempted by using the PF-PPP-*n* photocatalyst. However, neither visible-light nor UV-light irradiation induced photo-hydroxylation of benzene. A small amount of phenol was detected after 3 h of UV irradiation (phenol, 1.0 μmol/3 h) when F-PPS-*n* was employed as a photocatalyst. As expected,

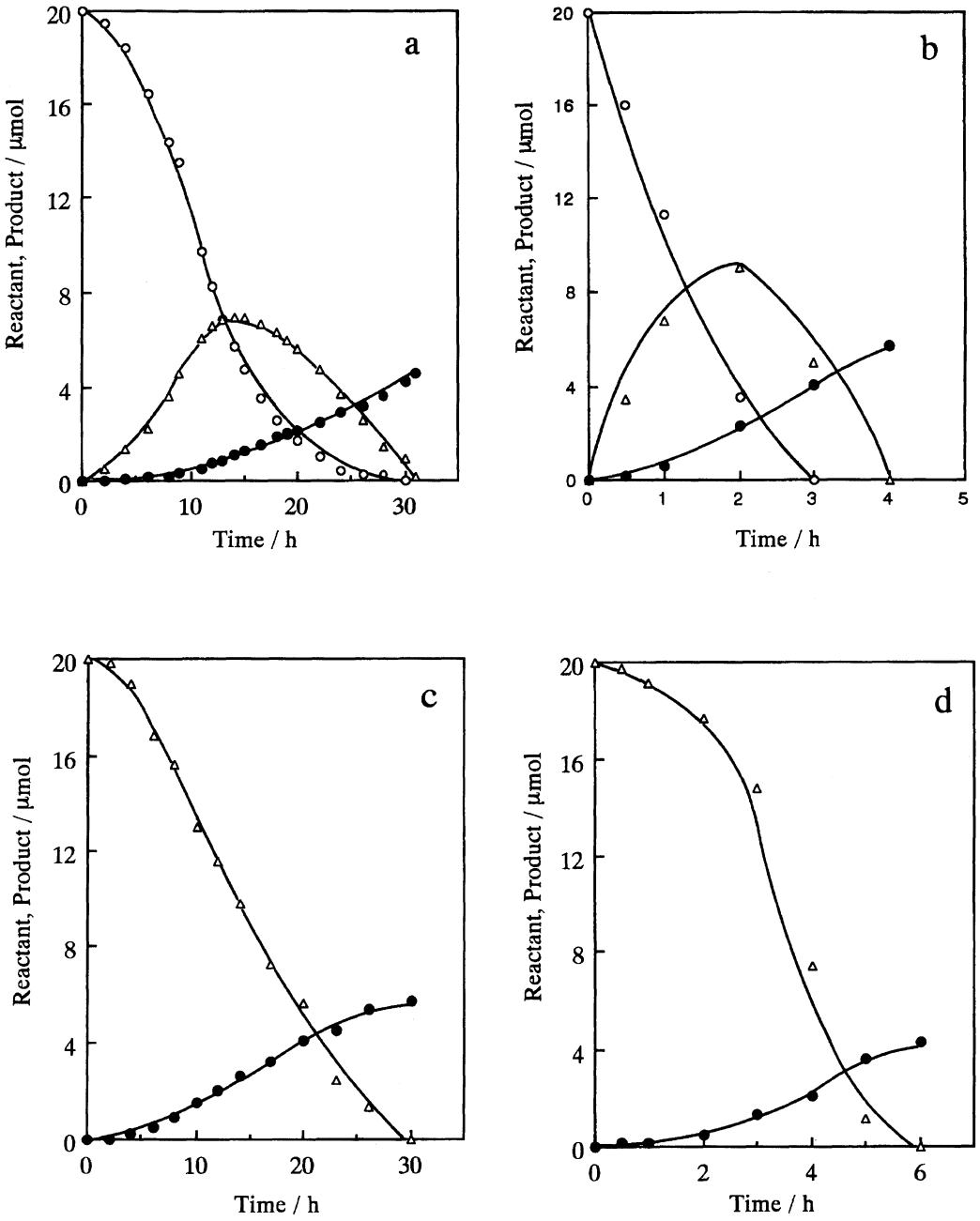

Fig. 5. Time-conversion plots for the PF-PPP-*n*-catalyzed photoreduction of dimethyl maleate (a) in methanol; (b) in acetonitrile, of dimethyl fumarate (c) in methanol; (d) in acetonitrile: (○) dimethyl maleate; (△) dimethyl fumarate; (●) dimethyl succinate.

F-PPP-*n*-catalyzed effective photooxidation of benzene to phenol under the same conditions (phenol, 17 μmol/3 h).

Mechanism of PF-PPP-*n*-Catalyzed Photoreduction. PF-PPP-*n* is considered to function as a novel photocatalyst in a similar mechanism to that proposed for PPP-*n*[6a] (Scheme 6), i.e., 1) photoexcited PF-PPP-*n* being converted to its anion radical (PF-PPP-$n^{-\bullet}$) by quenching its excited state with TEA and 2) the resulting radical anion reducing water to H_2 through colloidal noble metals like Ru or Rh as electron mediators.

In order to clarify the mechanism of the photoreduction of ketones and olefins, the photolysis of dimethyl maleate and fumarate was carried out in methanol–O–D or in acetonitrile containing D_2O (1.0 vol%). The unreacted substrates and the succinate were analyzed by GC-mass spectroscopy at 50% conversion. In Table 4 the relative intensities of molecular ion peaks of the reactant and products are summarized. It has been

Table 3. *p*-Phenylene Derivatives-Catalyzed Photoreduction of Aromatic Ketones in Methanol with TEA[a)]

R^1–CO–R^2		$-E^{red}_{1/2}$/V	Catalyst	Conversion/%	Yield[b)]/%	
R^1	R^2				Alcohol	Pinacol
Ph	CO_2Me	1.13[c)]	PPS-*n*	0	0	0
			F-PPS-*n*	34	54	Trace
			PPP-*n*	98[d)]	74	Trace
			PF-PPP-*n*	100[d)]	100	Trace
2-Pyridyl	2-Pyridyl	1.46[e)]	PPS-*n*	0	0	0
			F-PPS-*n*	8	Trace	0

a) Irradiated with λ>400 nm for 6 h. b) Based on the substrate converted. c) Polarographic half-wave reduction potentials in Volts vs. SCE in methanol. See Ref. 6b. d) Irradiated with λ>400 nm for 3 h. e) Polarographic half-wave reduction potentials in Volts vs. $Ag/AgNO_3$ in methanol. See Ref. 9a.

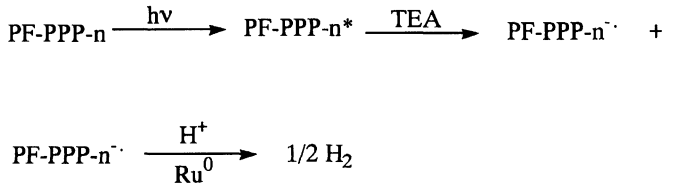

Scheme 6.

Table 4. Deuterium Isotopic Distribution in Recovered Substrates and Reaction Products after PF-PPP-*n*-Catalyzed Photolysis by Irradiation with λ>400 nm in Methanol or Acetonitrile[a)]

Solvent	Substrate	Deuterium content[b)]/%										
		Maleate(cis)			Fumarate(trans)			Succinate				
		d^0	d^1	d^2	d^0	d^1	d^2	d^0	d^1	d^2	d^3	d^4
MeOH	Maleate	100			60	20	20	7	17	36	28	13
	Fumarate				7	48	45	4	10	32	35	19
MeCN	Maleate	100			82	9	9	4	11	35	31	20
	Fumarate				15	50	35	10	23	33	26	8

a) Analyzed when the conversion is 50%. b) Determined by GC-MS analysis.

found that deuterium was bound to succinate and the fumarate, and that no deuterium was incorporated in the recovered maleate. These results strongly suggest that the photoreduction should proceed to give one-electron-transfer reduction intermediates (**7**) and (**8**), and that the disproportionation of (**8**) should eventually give the two-electron-transfer reduction product, the succinate (**9**) and the fumarate (**6**) as shown in Scheme 7 as was found for the PPP-*n*-catalyzed photoreduction and photoisomerization.[6a,9b,9c)]

The disproportionation mechanism does not seem consistent with the sequential reduction of carbonyl compounds to alcohols without formation of pinacols for the photoreaction in acetonitrile. In addition, the carbonyl compounds whose reduction potentials are positive enough to be reducible by the PF-PPP-*n* radical anions were photoreduced exclusively to alcohols (see Table 2). These facts imply that intermediary radical anions should also be positive enough to receive a second electron from the PF-PPP-*n* radical anion. In order to investigate the effect of the PF-PPP-*n* radical anion concentration on the photoreduction in acetonitrile, the photoreduction was examined using different the concentrations of PF-PPP-*n*. Figure 6 shows a sequence of photoreductions of 4-chlorobenzophenone with TEA in acetonitrile in the presence of different quantities of PF-PPP-*n* (a: 10 mg, b: 5 mg, c: 1 mg). Surprisingly, the concentration of PF-PPP-*n* photocatalyst affect not only the efficiency but also the distribution of the reduction products. These facts indicate that the effective formation of the PF-PPP-*n* radical anion should lead to successive reduction of the substrates and their intermediary radical anions, exclusively leading to a two-electron-transfer. On the other hand, a low concentration of PF-PPP-*n* radical anion due to a low concentration of the photocatalyst or an ineffective formation (which might be the case in the photolysis in methanol) should result in the disproportionation of the intermediary radicals derived from the one-electron-transfer reduction. Some side reactions seem to prevail in the latter case, leading to the formation of unidentified products as obvious from the discrepancy in the material balances,

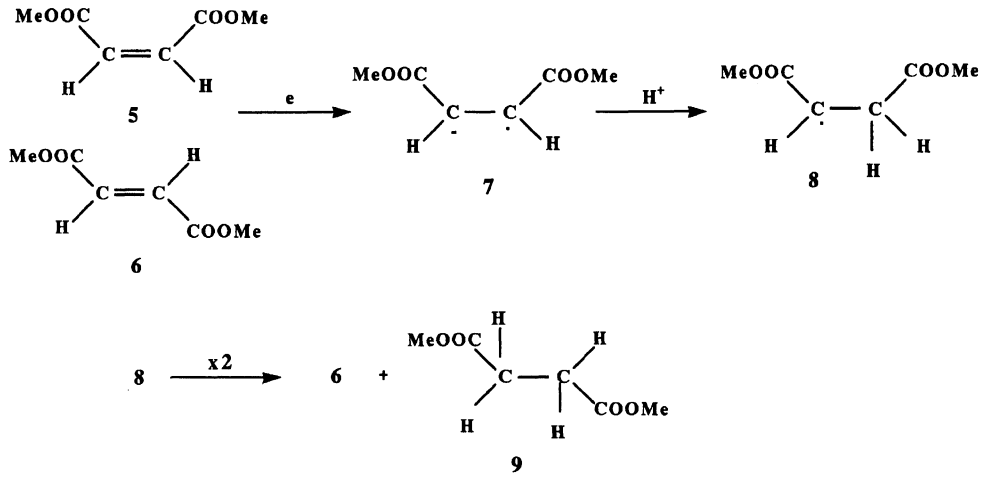

Scheme 7.

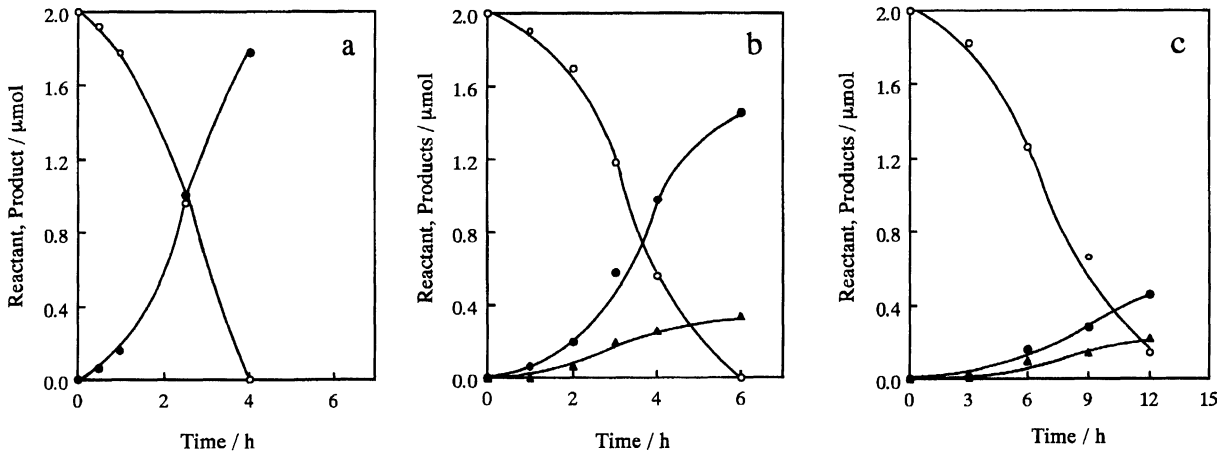

Fig. 6. Time-conversion plots for the PF-PPP-*n*-catalyzed photoreduction of 4-chlorobenzophenone in acetonitrile with PF-PPP-*n*, 10 mg (a), 5 mg (b), and 1 mg (c): (○) 4-chlorobenzophenone, (●) 4-chlorobenzhydrol, (▲) 4-chlorobenzpinacol.

which were observed in the photolysis with low concentration of PF-PPP-*n*, and in the photolysis of the maleate and fumarate.

Semiempirical Molecular Orbital Calculations. The molecules consisting of 3 monomer units (denoted by PF-OPP-3 and F-OPS-3) were regarded as model compounds for each photocatalyst (Scheme 8). In Table 5 the results of calculations of the neutral molecule, the anion radical, and the cation radical are summarized for the partially fluorinated *p*-terphenyl (PF-OPP-3) and perfluorinated *p*-terphenylene sulfide (F-OPS-3).

(a) Optimized Structures: The optimized structures of PF-OPP-3 and F-OPS-3 are shown in Fig. 7. For PF-OPP-3, the dihedral angles between the two phenylene rings are about 50°, which are smaller than those of F-OPP-3 and close to those of OPP-3. This can be ascribed to reduction of the steric repulsion between fluorine atoms at the ortho positions on the neighboring phenylene rings, nicely explaining the shift of the absorption of PF-PPP-*n* to the visible region.

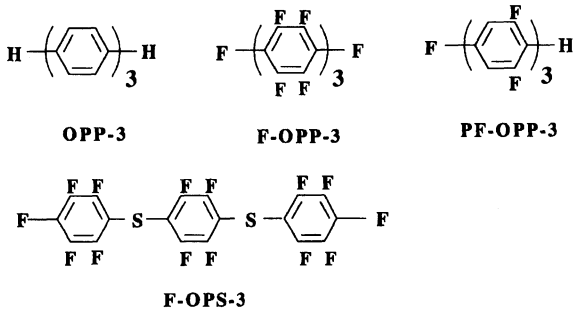

Scheme 8.

For the anion radicals, the dihedral angles of PF-OPP-3 are 37°, while those of F-OPP-3 and OPP-3 are 49° and 0.1°, respectively. The bond length between the phenylene rings (the C1–C1′ bond) in PF-OPP-3$^{-\bullet}$ are shortened, when compared with the neutral molecule. There is, however, no change in the C4′–C1″ bond length. This is in contrast to the results calculated for F-OPP-3, where both bonds are shortened.

Table 5. Computer-assisted Calculation of Anion Radicals and Cation Radicals of PF-OPP-3, F-OPP-3, OPP-3, and F-OPS-3[a)]

	Dihedral angles /degree	C–F Bond length/Å		Heat of formation /kcal mol^{-1}	Energy level/eV		
		C4–F	C3′–F		HOMO	LUMO	SOMO[b)]
OPP-3	50	—	—	72.7	−8.934	−0.351	
F-OPP-3	55	1.334	1.338	−510.1	−10.568	−2.211	
PF-OPP-3	50	1.352	1.354	−228.9	−9.532	−1.266	
F-OPS-3	—	1.333	1.338	−459.3	−9.883	−2.204	
OPP-3$^{-\cdot}$	0.1	—	—	46.7			−1.589
F-OPP-3$^{-\cdot}$	49	1.339	1.344	−570.6			−0.863
PF-OPP-3$^{-\cdot}$	37	1.347	1.350	−262.6			−0.566
F-OPS-3$^{-\cdot}$	—	1.338	1.343	−520.2			−0.002
OPP-3$^{+\cdot}$	0.8	—	—	260.1			−12.639
F-OPP-3$^{+\cdot}$	48	1.324	1.332	−276.2			−11.791
PF-OPP-3$^{+\cdot}$	37	1.344	1.350	−21.6			−10.624
F-OPS-3$^{+\cdot}$	—	1.324	1.332	−238.0			−11.512

a) See Experimental section. b) See Ref. 11.

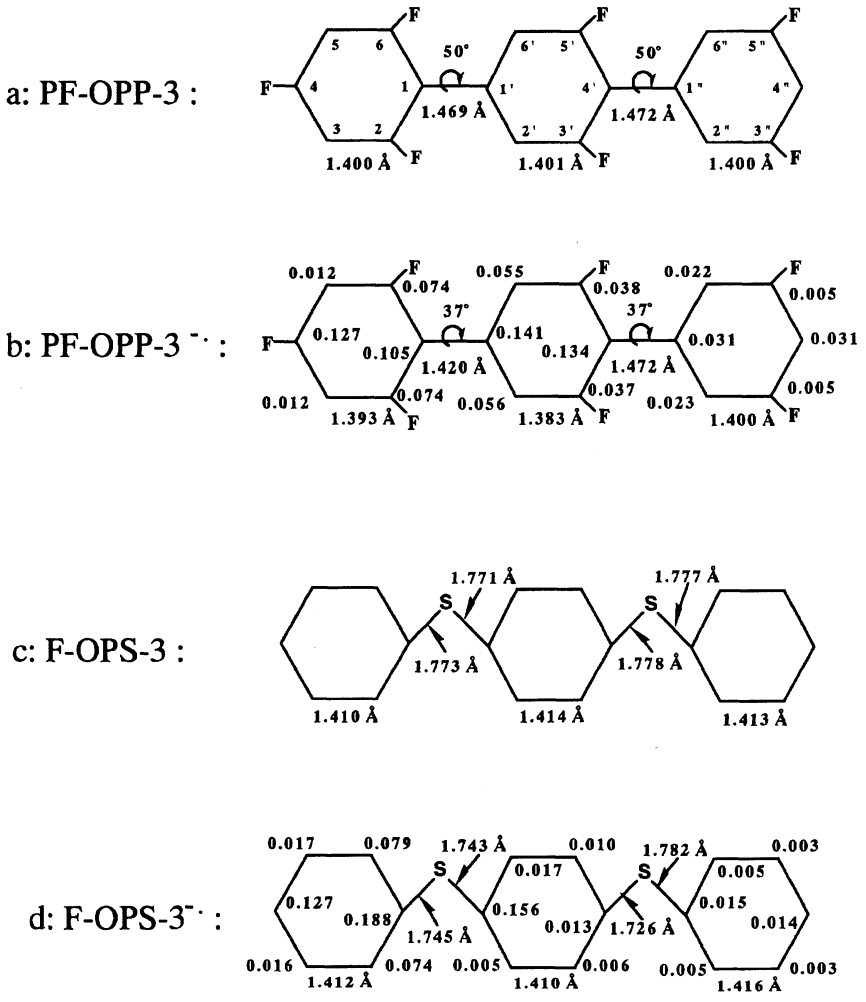

Fig. 7. Structures and spin densities of PF-OPP-3, PF-OPP-3$^{-\cdot}$, F-OPS-3, and F-OPS-3$^{-\cdot}$, calculated by using the MNDO/PM3 method. The C–C bond lengths and the torsion angles of the benzane rings are shown in Å and deg, respectively. For PF-OPP-3$^{-\cdot}$ and F-OPS-3$^{-\cdot}$, the spin densities on the carbon atoms are shown for each carbon atom.

Additionally, the C–C bonds in the phenylene rings parallel to the C1–C1′ bond (C2–C3, C5–C6, C2′–C3′, C5′–C6′) are also slightly shortened in the anion radical, but the both lengths of the C2″–C3″ and C5″–C6″ bonds do not change when compared with the neutral molecule. These facts imply that the anion radical might have a quinonoid-like structure of the central ring and the trifluorophenylene ring and the conjugation occurs only in these two phenylene rings. This partial conjugation is reflected in the spin distribution on the anion radical. It is interesting to note that higher spin densities are found on the carbons at positions C1 (0.105), C1′ (0.141), C4 (0.127), and C4′ (0.134). Thus the spin density is distributed mainly on the central ring and trifluorophenylene ring. It is in contrast to F-OPP-3 and OPP-3, the anion radicals of which show a quinonoid-like structure of the whole molecule.[1,7] This partial localization of the spin must be less in PF-PPP-*n*.

The C–C bonds of F-OPS-3$^{-\bullet}$, which are parallel to the longer axis of the molecule, are shorter in the central ring and longer in the terminal rings when compared to the neutral molecule. The C–S bonds of F-OPS-3$^{-\bullet}$ are shorter than those of the neutral molecule. The spin density of F-OPS-3$^{-\bullet}$ is distributed mainly between the carbons at the positions C1 (0.188), C1′ (0.156), C4 (0.127).

In the case of F-OPS-3, the C–F bond lengths are slightly longer for the anion radical (F-OPS-3$^{-\bullet}$) than for the neutral molecule, suggesting that the bond strength of the C–F bonds are weakened in F-OPS-3$^{-\bullet}$ as also observed for F-OPP-3$^{-\bullet}$.[1] On the other hand, the C–F bonds are slightly shorter in the anion radical than in the neutral molecule for PF-OPP-3. Therefore the C–F bonds are considered to be stable in PF-OPP-3$^{-\bullet}$, suggesting that this compound should be fairly resistant to chemical deterioration during the photocatalysis when PF-OPP-3$^{-\bullet}$ is involved as the intermediary species. This is consistent with the continued photocatalysis of PF-PPP-*n* for the reduction of water under UV irradiation.

(b) Activity in Photocatalysis: As shown in Table 6, the differences between the heats of formation for the neutral molecules and the anion radicals, which were obtained by MNDO/PM3 calculations are increasing in the order OPP-3, PF-OPP-3, and F-OPS-3 and F-OPP-3. These values imply an increasing thermodynamic stability of their anion radicals. In other words, the reducing ability of the anion radicals of these photocatalysts is higher in the opposite order. The order of the threshold values of the reduction potential for photoreduction of carbonyl compounds was found to be F-PPS-*n* (around −1.2 V vs. SCE in methanol), PF-PPP-*n* (−1.6 V), and PPP-*n* (−1.75 V). Therefore, the reducing abilities of the photocatalysts are well explained by the differences in the heat of formation of the neutral molecules and the anion radicals.

For the photocatalytic oxidation, the oxidizing power can also be evaluated using the heats of formation of the neutral molecule and its cation radical. In fact, F-OPP-3 and F-OPS-3, the model compounds for F-PPP-*n* and F-PPS-*n*, which were active for photooxidation of benzene to phenol, showed more positive values of the differences, which is consistent with their higher oxidizing power compared with PF-PPP-*n*.

Table 6. Differences between the Heat of Formation for the Neutral Molecules and the Ion Radicals

	ΔH_a/kcal mol^{-1} a)	ΔH_c/kcal mol^{-1} b)
OPP-3	−26.0	187.4
F-OPP-3	−60.5	233.9
PF-OPP-3	−41.4	207.3
F-OPS-3	−60.7	221.3

a) $\Delta H_a = H$(anion radical) − H(neutral molecule). See Table 5. b) $\Delta H_c = H$(cation radical) − H(neutral molecule). See Table 5.

HOMO and LUMO are also useful to evaluate the redox properties of phenylene compounds used as photocatalysts. The order of LUMO energies in Table 5 is −0.351 eV (OPP-3), −1.266 eV (PF-OPP-3), −2.204 eV (F-OPS-3), and −2.211 eV (F-OPP-3). This is consistent with the threshold values observed for the photoreduction of carbonyl compounds. Also the HOMO energies for the two compounds (F-OPP-3 and F-OPS-3) showing the oxidation of benzene to phenol are more positive than those of the other two compounds.

Conclusion

The partial fluorination of and/or the introduction of a –S– spacer into F-PPP-*n* caused a bathochromic shift of the onset of their absorption spectra, due to a relaxation of the steric repulsion between fluorine atoms on neighboring phenylene rings. We could predict the bathochromic shift by taking into account the dihedral angles between neighboring phenylene rings, which were calculated by semiempirical MO calculation using the MOPAC (MNDO/PM3 and MNDO/AM1) system.

Partially fluorinated poly(*p*-phenylene) showed an efficient visible-light-driven photocatalysis for the reduction of water, carbonyl compounds, and olefins in homogeneous system. On the other hand, the introduction of a sulfur spacer did not enhance the photocatalytic activity under visible-light irradiation. By taking account the redox potentials of these photocatalysts obtained from the MOPAC system, we could predict that photocatalytic activity of these molecules, and found that the photocatalytic activity can be controlled by introducing fluorine atoms in the phenylene units.

Experimental

Materials. 1-Bromo-2,4,6-trifluorobenzene and pentafluorobenzenethiol were obtained from Tokyo Kasei and were used without further purification. Hexafluorobenzene was obtained from Wako Pure Chemicals. Ketones were obtained from the following sources; benzophe-

none [Guaranteed reagent (GR)], 4-metoxybenzophenone (GR), 4-chlorobenzophenone (GR), and 4,4′-dimetoxybenzophenone (GR), from Nacalai Tesque, and 4,4′-dichlorobenzophenone (GR) from Wako Pure Chemical Industries. Methyl benzoylformate (GR), di-2-pyridyl ketone (GR) from Aldrich Chemical Company. *p*-Cyanobenzophenone was prepared by Friedel–Crafts reaction of 4-cyanobenzoyl chloride and benzene. Other chemicals used in this study were identical with those used in previous studies.[1,6,7]

Analysis. Gel permeation chromatographic (GPC) analysis was carried out by using a Tosoh G2000 H10 column (ϕ 7.6 mm×60 cm)×2 and an UV detector (at 254 nm) (Tosoh; UV-8000) on a Tosoh HLC-802UR. As eluent, THF was employed with a flow rate of 1.00 cm^3 min^{-1} at 40°C. Other analysis methods were identical with those reported in previous reports.[1,6,7]

Semiempirical MO Calculation. The calculations for OPP-3 were carried out by MOPAC Ver. 5.0 (QCPE No. 445), J. J. P. Stewart, "*QCPE Bull.* 1989, 9, 10,"; Tsuneo Hirano, "JCPE Newsletter, 1989," 1(2), 36; Revised as Ver. 5.01 by Jiro Toyoda, for OS/2 Personal Computers (NEC PC-9801), "JCPE Newsletter, 1990," 2(1), 56; those for F-OPP-3, PF-OPP-3, and F-OPS-3 were done by MOPAC Ver. 5.10 or 6.10 using CAChe system. Except for that neutral molecule and cation radical of PF-OPP-3 were calculated by using MNDO/AM1, the calculation was curried out by using MNDO/PM3.

Synthesis of PF-PPP-*n*. 1-Bromo-2,4,6-trifluorobenzene (5.0 g, 23.7×10^{-3} mol) in dry THF (5 ml) was added to magnesium turnings (0.59 g, 24.3×10^{-3} mol) in dry THF (5 ml) stirred on ice-bath. [$NiCl_2$(bpy)] was added to the resulting Grignard solution to start the polymerization. Smooth polymerization was observed and then refluxed over night. After the completion of the reaction, the reaction mixture was poured into a dilute HCl/methanol solution (20 ml) under ice-cooling. The polymer precipitated was collected by centrifugation. The precipitate was extracted with cyclohexane, the extract was evaporated and the residue was dissolved in methanol and reprecipitated by addition of water for purification. The resulting yellow precipitate (0.8 g) was dried and used as a photocatalyst. GPC analysis showed a broad peak at retention times between 25 to 40 min, followed by a series of sharp peaks at longer retention times, indicating that PF-PPP-*n* is a mixture of oligomers. Mass spectral analysis revealed that PF-PPP-*n* consist of oligomers from the trimer to at least the octamer, and that oligomers containing one bromine atom should contaminate PF-PPP-*n*. The oligomeric structure was also supported by broad ^{1}H NMR and ^{19}F NMR signals. The spectral data are shown below.

PF-PPP-*n*; IR (KBr) 3100, 2900, 1600, 1400, 1110, 1030, 1000, 840 cm^{-1}. ^{1}H NMR (600 MHz, THF-d_8) δ=6.57—7.88 (br). ^{19}F NMR (600 MHz, THF-d_8) δ=−48.08—−39.06 (m). MS, *m/z* 356 (*n*=3), 468 (*n*=4), 580 (*n*=5), 692 (*n*=6), 804 (*n*=7), 916 (*n*=8) (M^+). The longer oligomer (*n*>8) have not been analyzed due to the limit of the instrument.

Synthesis of F-PPS-*n*.[2] The potassium pentafluorobenzenethiolate (6.0 g, 25.2×10^{-3} mol) prepared from KOH and pentafluorobenzanethiol was added slowly to hexafluorobenzene (5.4 g, 29.0×10^{-3} mol) in pyridine (75 ml) and the mixture was stirred at reflux temperature for 1.5 h. The precipitated pale yellow powder was collected, thoroughly washed with water, and dried in vacuo (4.2 g). The resulting F-PPS-*n* was insoluble in all organic solvents.

F-PPS-*n*; IR (KBr) 1470, 1250, 960, 810 cm^{-1}. MS, *m/z* 1086 (*n*=6), 1266 (*n*=7), 1446 (*n*=8), 1626 (*n*=9), 1807 (*n*=10) (M^+). The longer oligomers (*n*>10) have not been analyzed due to the limit of the instrument.

Synthesis of F-PPP-*n*. The procedure was almost identical with the synthesis of perfluorinated *p*-terphenyl and *p*-quaterphenyl[1,4] except for the stoichiometry of the Grignard solution derived from pentafluorophenyl bromide and decafluorobiphenyl. Pentafluorophenylmagnesium bromide (5.43 g, 2.0×10^{-2} mol) was reacted with decafluorobiphenyl (2.70 g, 8.0×10^{-3} mol) in a dry THF (30 ml) at 60°C for about 12 h. The resulting white precipitate (4.0 g) was collected by filtration and thoroughly washed with water, then dried in vacuo. The resulting F-PPP-*n* was insoluble in all organic solvents.

F-PPP-*n*; IR (KBr) 1460, 1240, 1120, 960, 710 cm^{-1}. MS, *m/z* 482 (*n*=3), 630 (*n*=4), 778 (*n*=5), 926 (*n*=6), 1074 (*n*=7), 1222 (*n*=8), 1370 (*n*=9), 1518 (*n*=10) (M^+). The longer oligomer (*n*>10) have not been analyzed due to the limit of the instrument.

Photoreduction of H_2O to H_2. As reported in previous papers,[1,6,7] PF-PPP-*n* or F-PPS-*n* (10 mg) was added to a mixture of water (0.5 ml, 2.78×10^{-2} mol), TEA (0.5 ml, 3.58×10^{-3} mol), and methanolic $RuCl_3$ solution (0.5 ml, 6.0×10^{-3} mol dm^{-3}) in a Pyrex tube (8 mm in diameter). The resulting suspension was flashed with argon gas under ice-cooling, closed off with a gum stopper, and then irradiated under magnetic stirring at λ>400 nm by using a 300 W halogen lamp fitted with a sodium nitrite solution filter. The gaseous and liquid products were analyzed by GLC as reported previously.[1,6,7]

Other PF-PPP-*n*-catalyzed photoreductions were conducted in identical procedures as used in previous studies; the procedure of photoreduction of aromatic ketones can be found referring to our previous PPP-*n*-catalyzed photoreduction,[6a] photooxidation of benzene is described in the preceding paper.[1]

Determination of Deuterium Isotopic Distribution. Photoreductions of dimethyl maleate and dimethyl fumarate were performed in methanol-*O-D* and in acetonitrile containing D_2O under the same conditions as described above. When 50% of the substrate disappeared, the irradiation was stopped, and then the reaction solution were analyzed by GC-MS.

This research was supported by a grant-in-aid for Scientific Research Nos. 04203119, 04455017 from the Ministry of Education, Science and Culture. The research was also conducted as a project of the Research Society of CO_2-Fixation sponsored by the Institute of Laser Technology under the commission of the Kansai Electric Power Company, Inc. Additional financial aid provided by RITE, the Shorai Foundation for Science and Technology, and Nagase Science and Technology Foundation are also gratefully acknowledged. The author wishes to thank Dr. Dieter Meissner (a visiting Scientist supported by RITE, Institute für Solarenergieforschung, Hannover) for his kind suggestion.

References

1) K. Maruo, Y. Wada, and S. Yanagida, *Bull. Chem. Soc. Jpn.*, **65**, 3439 (1992).

2) P. Robson, M. Stacey, R. Stephens, and J. C. Tatlow, *J. Am. Chem. Soc.*, **82**, 4754 (1960).

3) T. Yamamoto, Y. Hayashi, and A. Yamamoto, *Bull. Chem. Soc. Jpn.*, **51**, 2091 (1978).

4) J. L. Cotter, G. J. Knight, J. M. Lancaster, and W. W. Wright, *J. Appl. Polym. Sci.*, **12**, 2481 (1968).

5) a) A. J. Bilbo and G. M. Wyman, *J. Am. Chem. Soc.*, **75**, 5312 (1953); b) D. E. Fenton, *Chem. Ind. (London)*, **24**, 695 (1969); c) W. Zapka and U. Brackmann, *Appl. Phys.*, **20**, 283 (1979).

6) a) T. Shibata, A. Kabumoto, T. Shiragami, O. Ishitani, C. Pac, and S. Yanagida, *J. Phys. Chem.*, **94**, 2068 (1990); b) S. Matsuoka, T. Kohzuki, Y. Kuwana, A. Nakamura, and S. Yanagida, *J. Chem. Soc., Perkin Trans. 2*, **1992**, 679.

7) S. Matsuoka, H. Fujii, T. Yamada, C. Pac, A. Ishida, S. Takamuku, M. Kusaba, N. Nakashima, S. Yanagida, K. Hashimoto, and T. Sakata, *J. Phys. Chem.*, **95**, 5802 (1991).

8) a) T. Shiragami, C. Pac, and S. Yanagida, *J. Phys. Chem.*, **94**, 504 (1990); b) P. Zuman, O. Exner, R. F. Rekker, and W. T. Nauta, *Collect. Czech. Chem. Commun.*, **33**, 3213 (1968); c) P. J. Wagner, R. J. Truman, A. E. Puchalski, and R. Wake, *J. Am. Chem. Soc.*, **108**, 7727 (1986).

9) a) O. Ishitani, S. Yanagida, S. Takamuku, and C. Pac, *J. Org. Chem.*, **52**, 2790 (1987); b) C. Pac, M. Ihama, M. Yasuda, Y. Miyauchi, and H. Sakurai, *J. Am. Chem. Soc.*, **103**, 6495 (1981); c) C. Pac, Y. Miyauchi, O. Ishitani, M. Ihama, M. Yasuda, and H. Sakurai, *J. Org. Chem.*, **49**, 26 (1984).

10) As unidentified products, the coupling products of the radical from TEA, $CH_3\dot{C}HN(Et)_2$, with the intermediary radicals produced from maleate or fumarate are conceivable.

11) The energy levels of SOMOs are also useful for comparison of the redox abilities of the photocatalysts. However, the order of the energy levels of SOMOs in the anion radicals and the cation radicals were not consistent with those of the redox ability of the photocatalysts especially when *p*-phenylene and its fluorinated derivatives were compared.